

Temperature dependence of mode coupling effect in piezoelectric vibrator made of $[001]_c$-poled Mn-doped 0.24PIN-0.46PMN-0.30PT ternary single crystals with high electromechanical coupling factor

Nai-Xing Huang(黄乃兴), En-Wei Sun(孙恩伟), Rui Zhang(张锐), Bin Yang(杨彬), Jian Liu(刘俭), Tian-Quan Lü(吕天全), Wen-Wu Cao(曹文武)

Citation: Chin. Phys. B . 2020, 29(7): 075201 . **doi:** 10.1088/1674-1056/ab8a3e
Journal homepage: http://cpb.iphy.ac.cn; http://iopscience.iop.org/cpb

What follows is a list of articles you may be interested in

Harvesting base vibration energy by a piezoelectric inverted beam with pendulum

Jia-Nan Pan(潘家楠), Wei-Yang Qin(秦卫阳), Wang-Zheng Deng(邓王蒸), Hong-Lei Zhou(周红磊)

Chin. Phys. B . 2019, 28(1): 017701 . **doi:** 10.1088/1674-1056/28/1/017701

Hybrid temperature effect on a quartz crystal microbalance resonator in aqueous solutions

Qiang Li(李强), Yu Gu(谷宇), Bin Xie(谢斌)

Chin. Phys. B . 2017, 26(6): 067704 . **doi:** 10.1088/1674-1056/26/6/067704

Stoney formula for piezoelectric film/elastic substrate system

Wang-Min Zhou(周旺民), Wang-Jun Li(李望君), Sheng-Yun Hong(洪圣运), Jie Jin(金杰), Shu-Yuan Yin(尹姝媛)

Chin. Phys. B . 2017, 26(3): 037701 . **doi:** 10.1088/1674-1056/26/3/037701

Resonance-mode effect on piezoelectric microcantilever performance in air, with a focus on the torsional modes

Qiu Hua-Cheng, Dara Feili, Wu Xue-Zhong, Helmut Seidel

Chin. Phys. B . 2014, 23(2): 027701 . **doi:** 10.1088/1674-1056/23/2/027701

Permittivity and its temperature dependence in hexagonal structure BN dominated by the local electric field

Zhang Ting, Wu Meng-Qiang, Zhang Shu-Ren, Xiong Jie, Wang Jin-Ming, Zhang Da-Hai, He Feng-Mei, Li Zhong-Ping

Chin. Phys. B . 2012, 21(7): 077701 . **doi:** 10.1088/1674-1056/21/7/077701

Temperature dependence of mode coupling effect in piezoelectric vibrator made of $[001]_c$-poled Mn-doped 0.24PIN–0.46PMN–0.30PT ternary single crystals with high electromechanical coupling factor*

Nai-Xing Huang(黄乃兴)[1,2,†], En-Wei Sun(孙恩伟)[2,3,‡], Rui Zhang(张锐)[2], Bin Yang(杨彬)[2], Jian Liu(刘俭)[2], Tian-Quan Lü(吕天全)[2], and Wen-Wu Cao(曹文武)[2,3]

[1] *Department of Physics, Northeast Petroleum University, Daqing* 163318, *China*
[2] *The School of Instrumentation Science and Engineering, Harbin Institute of Technology, Harbin* 150001, *China*
[3] *Department of Mathematics and Materials Research Institute, The Pennsylvania State University, University Park, PA* 16802, *USA*

(Received 22 February 2020; revised manuscript received 10 April 2020; accepted manuscript online 17 April 2020)

The influence of temperature on mode coupling effect in piezoelectric vibrators remains unclear. In this work, we discuss the influence of temperature on two-dimensional (2D) mode coupling effect and electromechanical coupling coefficient of cylindrical $[001]_c$-poled Mn-doped 0.24PIN–0.46PMN–0.30PT piezoelectric single-crystal vibrator with an arbitrary configuration ratio. The electromechanical coupling coefficient k_t decreases with temperature increasing, whereas k_{33} is largely invariant in a temperature range of 25 °C–55 °C. With the increase of temperature, the shift in the 'mode dividing point' increases the scale of the poling direction of the piezoelectric vibrator. The temperature has little effect on coupling constant Γ. At a given temperature, the coupling constant Γ of the cylindrical vibrator is slightly greater than that of the rectangular vibrator. When the temperature changes, the applicability index (M) values of the two piezoelectric vibrators are close to 1, indicating that the coupling theory can be applied to piezoelectric vibrators made of late-model piezoelectric single crystals.

Keywords: mode coupling effect, piezoelectric vibrator, piezoelectric single crystal, temperature dependence

PACS: 52.35.Mw, 77.65.–j, 77.65.Fs, 77.84.–s **DOI:** 10.1088/1674-1056/ab8a3e

1. Introduction

The analysis of the coupling between the vibration modes of a piezoelectric vibrator is vital to the design of practical devices such as piezoelectric sensors, piezoelectric actuators, and ultrasonic transducers. The most common problem is the coupling analysis between the vibration mode along the poling direction and that perpendicular to the poling direction. The electromechanical coupling coefficient of piezoelectric material along the poling direction in the vibration mode has been extensively discussed. The material parameters, including the elastic, dielectric, and piezoelectric constants, vary with temperature. Therefore, the coupling between the two vibration modes and the electromechanical coupling are affected by temperature. Piezoelectric vibrators are the basic components of piezoelectric devices. Rectangular and cylindrical piezoelectric vibrators with different configuration ratios are the most common examples.

In recent years, $PbIn_{1/2}Nb_{1/2}O_3$–$PbMg_{1/3}Nb_{2/3}O_3$–$PbTiO_3$ (PIN–PMN–PT) ternary single crystals have attracted considerable attention owing to their high phase transition temperatures ($T_{R-T} > 120$ ℃) and good temperature stabilities, making them suitable for being used in electromechanical devices in a wide range of temperatures.[1,2] Doping with Mn can improve some of the physical properties of ferroelectrics.[3] The mechanical quality factor (Q_M) of Mn-doped PIN–PMN–PT (Mn:PIN–PMN–PT) ternary single crystals poled along the $[001]_c$ pseudo-cubic direction can be as high as 1000, which is comparable to that of hard $PbZrTiO_3$-type (PZT) ceramics.[4] Currently, the applications of piezoelectric materials are not limited to conventional environments,[5,6] such as room temperature condition environments. The mode-coupling effect in rectangular beams made of 0.33PIN–0.35PMN–0.32PT ternary single crystals has been studied at room temperature.[7] However, the influence of temperature on the mode coupling effect in a rectangular beam is unclear. Furthermore, there is no research on the mode coupling effect in ternary, cylindrical PIN–PMN–PT single-crystal resonator.

In this study, we analyze the mode coupling effects in rectangular piezoelectric vibrator and cylindrical piezoelectric

*Project supported by the Basic Scientific Research Foundation of College and University in Heilongjiang Province, China (Grant No. 2018QNL-16), the Guiding Science and Technology Project of Daqing City (GSTPDQ), China (Grant No. zd-2019-03), and the National Natural Science Foundation of China (Grant Nos. 11304061 and 51572056).

†Corresponding author. E-mail: huangnaixing@163.com
‡Corresponding author. E-mail: sunew@hit.edu.cn

© 2020 Chinese Physical Society and IOP Publishing Ltd

vibrator, both are made of $[001]_c$-poled Mn-doped 0.24PIN–0.46PMN–0.30PT ternary single crystal, in a temperature range of 25 ℃–55 ℃. In addition, we derive an equation for the electromechanical coupling coefficient k_t of Mn:PIN–PMN–PT ternary single crystal as a function of temperature. This study will be helpful in designing Mn:PIN–PMN–PT-based devices.

2. Theory

Figure 1 shows schematically two piezoelectric vibrators made of $[001]_c$-poled Mn-doped 0.24PIN–0.46PMN–0.30PT single-crystal material. The z axis is the poling direction for both of the resonators, and the four surfaces normal to the z axis are covered by the electrodes.

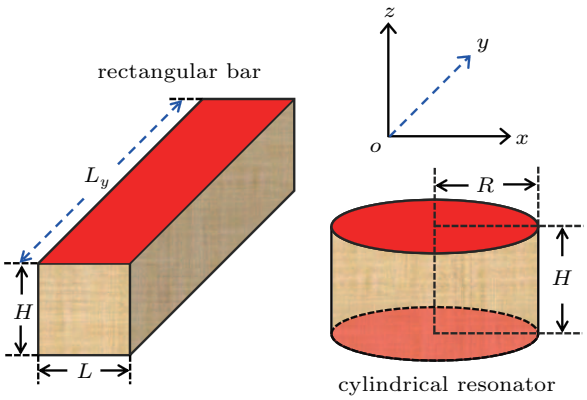


Fig. 1. Schematic diagram of piezoelectric vibrators and their coordinate system.

For the rectangular vibrator, we assume that the bar extends infinitely in the y-axis direction. Thus, the rectangular vibrator exhibits two-dimensional coupled vibrations in the x and z directions.[8–10] The configuration ratio G is defined as $G = L/H$, where H is in the poling direction of the vibrator. The theoretical relationship for the coupled vibration is[8,9,11]

$$(f_x^2 - f^2)(f_z^2 - f^2) = f_x^2 f_z^2 \Gamma_1^2, \tag{1}$$

where f_x and f_z are the resonant frequency in the x and z directions without any mode coupling, respectively, and Γ_1 is a coupling constant. For a rectangular piezoelectric vibrator, four limiting resonant frequency constants, namely $f_l H$, $f_L H$, $f_h H$, and $f_H H$ are respectively defined as follows:[8,9]

$$f_l H = \frac{1}{2G}\sqrt{\frac{c_{11}^{\mathrm{E}}}{\rho}}, \tag{2}$$

$$f_L H = \frac{1}{2G}\sqrt{\frac{c_{11}^{\mathrm{E}}(1-\alpha^2)}{\rho}}, \tag{3}$$

$$f_h H = \frac{X_t}{\pi}\sqrt{\frac{c_{33}^{\mathrm{D}}}{\rho}}, \tag{4}$$

$$f_H H = \frac{X_t^*}{\pi}\sqrt{\frac{c_{33}^{\mathrm{D}*}}{\rho}}, \tag{5}$$

where

$$\alpha = \Gamma_1 = \frac{c_{13}^{\mathrm{E}}}{\sqrt{c_{11}^{\mathrm{E}} c_{33}^{\mathrm{E}}}}, \tag{6}$$

$$c_{33}^{\mathrm{D}} = c_{33}^{\mathrm{E}} + \frac{e_{33}^2}{\varepsilon_{33}^S} = \frac{c_{33}^{\mathrm{E}}}{1-k_t^2}, \tag{7}$$

$$c_{33}^{\mathrm{D}*} = c_{33}^* + \frac{(e_{33}^*)^2}{\varepsilon_{33}^*} = \frac{c_{33}^*}{1-(k_t^*)^2} = \frac{c_{33}^{\mathrm{E}}(1-\alpha^2)}{1-(k_t^*)^2}. \tag{8}$$

In Eqs. (7) and (8),

$$c_{33}^* = c_{33}^{\mathrm{E}} - \frac{(c_{13}^{\mathrm{E}})^2}{c_{11}^{\mathrm{E}}} = c_{33}^{\mathrm{E}}(1-\alpha^2), \tag{9}$$

$$e_{33}^* = e_{33} - \frac{e_{31} c_{13}^{\mathrm{E}}}{c_{11}^{\mathrm{E}}}, \tag{10}$$

$$\varepsilon_{33}^* = \varepsilon_{33}^S + \frac{e_{31}^2}{c_{11}^{\mathrm{E}}}, \tag{11}$$

$$k_t^2 = \frac{e_{33}^2}{c_{33}^{\mathrm{D}} \varepsilon_{33}^S}, \tag{12}$$

$$(k_t^*)^2 = \frac{(e_{33}^*)^2}{c_{33}^{\mathrm{D}*} \varepsilon_{33}^*}, \tag{13}$$

and X_t and X_t^* are, respectively, the lowest nonzero positive roots of

$$\begin{cases} 1 - k_t^2 \dfrac{\tan X}{X} = 0, \\ 1 - (k_t^*)^2 \dfrac{\tan X^*}{X^*} = 0. \end{cases} \tag{14}$$

From Eqs. (2) and (3), we obtain

$$\frac{f_L}{f_l} = \sqrt{1-\alpha^2}, \tag{15}$$

and from Eqs. (4) and (5), we have

$$\frac{f_H}{f_h} = \frac{X_t^*}{X_t}\sqrt{\frac{c_{33}^{\mathrm{D}*}}{c_{33}^{\mathrm{D}}}} = M_1\sqrt{1-\alpha^2}, \tag{16}$$

where

$$M_1 = \frac{f_H/f_h}{f_L/f_l} = \frac{X_t^*}{X_t}\sqrt{\frac{1-k_t^2}{1-(k_t^*)^2}}. \tag{17}$$

The factor M_1 is the applicability index, which is a measure of the internal consistency in the application of the coupling theory.[8,9] If $M_1 = 1$, from Eqs. (15) and (16), we have

$$\frac{f_H}{f_h} = \frac{f_L}{f_l} = \sqrt{1-\alpha^2}. \tag{18}$$

By substituting Eqs. (2)–(5) into Eq. (1), we obtain the following solutions:

$$f_1 H = \sqrt{\frac{c_{33}^{\mathrm{D}} X_{\mathrm{t}}^2}{2\rho\pi^2} + \frac{c_{11}^{\mathrm{E}}}{8\rho G^2} + \frac{\sqrt{16(c_{33}^{\mathrm{D}})^2 X_{\mathrm{t}}^4 G^4 - 8c_{11}^{\mathrm{E}} c_{33}^{\mathrm{D}} X_{\mathrm{t}}^2 \pi^2 (1-2\Gamma_1^2) G^2 + (c_{11}^{\mathrm{E}})^2 \pi^4}}{8\rho\pi^2 G^2}}, \tag{19}$$

$$f_2 H = \sqrt{\frac{c_{33}^{\mathrm{D}} X_{\mathrm{t}}^2}{2\rho\pi^2} + \frac{c_{11}^{\mathrm{E}}}{8\rho G^2} - \frac{\sqrt{16(c_{33}^{\mathrm{D}})^2 X_{\mathrm{t}}^4 G^4 - 8c_{11}^{\mathrm{E}} c_{33}^{\mathrm{D}} X_{\mathrm{t}}^2 \pi^2 (1-2\Gamma_1^2) G^2 + (c_{11}^{\mathrm{E}})^2 \pi^4}}{8\rho\pi^2 G^2}}. \tag{20}$$

For the cylindrical resonator shown in Fig. 1, the piezoelectric vibrator exhibits two-dimensional coupled vibration in the radial and z-axis direction. In this case, the configuration ratio G is defined as $G = H/R$, where H is in the poling direction of the piezoelectric single crystal. The theoretical equation for the coupled vibration is[8,12]

$$(f_{\mathrm{r}}^2 - f^2)(f_z^2 - f^2) = f_{\mathrm{r}}^2 f_z^2 \Gamma_2^2, \tag{21}$$

where f_{r} and f_z are the resonant frequency in the radial and z-axis direction without any coupling, respectively, and Γ_2 is the coupling constant. For a cylindrical piezoelectric vibrator, the four limiting resonant frequency constants, namely $f_{\mathrm{r}}H$, $f_{\mathrm{R}}H$, $f_{\mathrm{t}}H$, and $f_{\mathrm{T}}H$ can be respectively defined as follows:[8,13]

$$f_{\mathrm{r}} H = \frac{G\zeta_1}{2\pi}\sqrt{\frac{c_{11}^{\mathrm{E}}}{\rho}}, \tag{22}$$

$$f_{\mathrm{R}} H = \frac{G\zeta_1^{\mathrm{P}}}{2\pi}\sqrt{\frac{c_{11}^{\mathrm{E}}(1-\alpha^2)}{\rho}}, \tag{23}$$

$$f_{\mathrm{t}} H = \frac{X_{\mathrm{t}}}{\pi}\sqrt{\frac{c_{33}^{\mathrm{D}}}{\rho}}, \tag{24}$$

$$f_{\mathrm{T}} H = \frac{X_{33}}{\pi}\sqrt{\frac{1}{\rho s_{33}^{\mathrm{E}}(1-k_{33}^2)}}, \tag{25}$$

where ζ_1 is the first positive root of Bessel functions and satisfies

$$\frac{\zeta \mathrm{J}_0(\zeta)}{\mathrm{J}_1(\zeta)} = 1 - \gamma, \tag{26}$$

and ζ_1^{P} is the first positive root of

$$\frac{\zeta^{\mathrm{P}} \mathrm{J}_0(\zeta^{\mathrm{P}})}{\mathrm{J}_1(\zeta^{\mathrm{P}})} = \frac{1-\gamma}{1-\alpha^2}, \tag{27}$$

where

$$\gamma = c_{12}^{\mathrm{E}}/c_{11}^{\mathrm{E}}, \tag{28}$$

$$k_{33}^2 = \frac{d_{33}^2}{s_{33}^{\mathrm{E}}\varepsilon_{33}^{\mathrm{T}}}, \tag{29}$$

and X_{33} is the lowest nonzero positive root of

$$1 - k_{33}^2 \frac{\tan X}{X} = 0. \tag{30}$$

From Eqs. (22) and (23), we obtain

$$\frac{f_{\mathrm{R}}}{f_{\mathrm{r}}} = \frac{\zeta_1^{\mathrm{P}}}{\zeta_1}\sqrt{1-\alpha^2}, \tag{31}$$

and from Eqs. (24) and (25), we have

$$\begin{aligned}\frac{f_{\mathrm{T}}}{f_{\mathrm{t}}} &= \frac{X_{33}}{X_{\mathrm{t}}}\sqrt{\frac{1}{c_{33}^{\mathrm{D}} s_{33}^{\mathrm{E}}(1-k_{33}^2)}} \\ &= \frac{X_{33}}{X_{\mathrm{t}}}\sqrt{\frac{1-k_{\mathrm{t}}^2}{1-k_{33}^2}}\sqrt{1-\beta^2}\sqrt{1-\alpha^2},\end{aligned} \tag{32}$$

where

$$\beta^2 = \frac{\alpha^2(1-\gamma)}{(1-\alpha^2)(1+\gamma)}, \tag{33}$$

$$M_2 = \frac{f_{\mathrm{T}}/f_{\mathrm{t}}}{f_{\mathrm{R}}/f_{\mathrm{r}}} = \frac{\zeta_1}{\zeta_1^{\mathrm{P}}}\sqrt{1-\beta^2}\frac{X_{33}}{X_{\mathrm{t}}}\sqrt{\frac{1-k_{\mathrm{t}}^2}{1-k_{33}^2}}. \tag{34}$$

For the cylindrical resonator, the coupling constant Γ_2 is given by

$$\Gamma_2 = \sqrt{\left|(\zeta_1^{\mathrm{P}}/\zeta_1)^2(1-\alpha^2) - 1\right|}. \tag{35}$$

Solving Eq. (21) leads to the following solutions:

$$f_1 H = \sqrt{\frac{c_{33}^{\mathrm{D}} X_{\mathrm{t}}^2}{2\rho\pi^2} + \frac{c_{11}^{\mathrm{E}}\zeta_1^2 G^2}{8\rho\pi^2} + \frac{\sqrt{16(c_{33}^{\mathrm{D}})^2 X_{\mathrm{t}}^4 - 8c_{11}^{\mathrm{E}} c_{33}^{\mathrm{D}} X_{\mathrm{t}}^2 \zeta_1^2 (1-2\Gamma_2^2) G^2 + (c_{11}^{\mathrm{E}})^2 \zeta_1^4 G^4}}{8\rho\pi^2}}, \tag{36}$$

$$f_2 H = \sqrt{\frac{c_{33}^{\mathrm{D}} X_{\mathrm{t}}^2}{2\rho\pi^2} + \frac{c_{11}^{\mathrm{E}}\zeta_1^2 G^2}{8\rho\pi^2} - \frac{\sqrt{16(c_{33}^{\mathrm{D}})^2 X_{\mathrm{t}}^4 - 8c_{11}^{\mathrm{E}} c_{33}^{\mathrm{D}} X_{\mathrm{t}}^2 \zeta_1^2 (1-2\Gamma_2^2) G^2 + (c_{11}^{\mathrm{E}})^2 \zeta_1^4 G^4}}{8\rho\pi^2}}. \tag{37}$$

The $[001]_c$-poled Mn-doped 0.24PIN–0.46PMN–0.30PT piezoelectric single-crystal vibrator and $[001]_c$-poled PMN-0.30PT single-crystal resonator in Ref. [13] have the same macroscopic symmetry and vibration mode. For the cylindrical resonator with

an arbitrary configuration ratio $G = H/R$, the electromechanical coupling coefficient k^{eff} can be given by[12,13]

$$k^{\text{eff}} = \frac{d_{33} + \dfrac{2d_{31}s^{\text{E}}_{13}}{(s^{\text{E}}_{11}+s^{\text{E}}_{12})}\left[g^2(G)-1\right]}{\sqrt{\left(s^{\text{E}}_{33} + \dfrac{2(s^{\text{E}}_{13})^2}{(s^{\text{E}}_{11}+s^{\text{E}}_{12})}\left[g^2(G)-1\right]\right)\left(\varepsilon^{\text{T}}_{33} + \dfrac{2d^2_{31}}{(s^{\text{E}}_{11}+s^{\text{E}}_{12})}\left[g^2(G)-1\right]\right)}}, \tag{38}$$

where

$$g(G) = \frac{G}{2}\frac{\zeta_1}{X_{\text{t}}}\sqrt{\frac{c^{\text{E}}_{11}}{c^{\text{D}}_{33}(1-\Gamma_2^2)}}\frac{f_2}{f_1}. \tag{39}$$

3. Results and discussion

Figure 2 shows the electromechanical coupling coefficient of the cylindrical resonator with an arbitrary configuration ratio at temperatures of 25 ℃, 40 ℃, and 55 ℃, obtained by using Eq. (38) and the $[001]_c$-poled Mn-doped 0.24PIN–0.46PMN–0.30PT single-crystal parameters derived from Ref. [4]. At a given temperature, the electromechanical coupling coefficient k^{eff} increases with configuration ratio $G = H/R$ increasing. When $G \to 0$, the electromechanical coupling coefficient k_{t} decreases with temperature rising. However, when $G \to \infty$, the electromechanical coupling coefficient k_{33} (~ 0.88) is largely invariant at temperatures ranging from 25 ℃ to 55 ℃ as shown in Table 1.

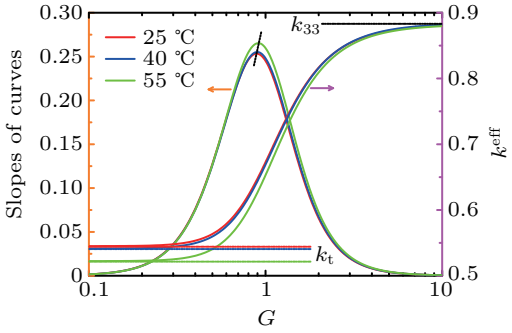


Fig. 2. Electromechanical coupling coefficient k^{eff} of cylindrical resonator with arbitrary configuration ratio at temperatures of 25 ℃, 40 ℃, and 55 ℃.

Table 1. Electromechanical coupling coefficients k_{t} and k_{33} of cylindrical resonator at different temperatures, including the slope peaks.

Temperature/℃	k_{t}	k_{33}	Slope peaks	
			$(G = H/R)$	Slope
25	0.5453	0.8831	0.89	0.2533
30	0.5445	0.8841	–	–
35	0.5442	0.8844	–	–
40	0.5412	0.8843	0.90	0.2552
45	0.5374	0.8843	–	–
50	0.5336	0.8839	–	–
55	0.5236	0.8824	0.91	0.2653

The electromechanical coupling factor k_{33} of the $[001]_c$-poled 0.28PIN–0.40PMN–0.32PT ternary single crystal increases from 0.91 at −50 ℃ to 0.94 at 125 ℃,[1] while that of the $[001]_c$-poled 0.26PIN–0.44PMN–0.30PT single crystals remains constant at 0.91 in a temperature range of −10 ℃–70 ℃.[2] Thus, the temperature may have little effect on the electromechanical coupling coefficient k_{33} of $[001]_c$-poled Mn-doped PIN–PMN–PT ternary single crystal in a temperature range of 25 ℃–55 ℃. The peaks of the curves move in the direction of greater configuration ratio G with temperature increasing as shown in Fig. 2 and Table 1. Listed in Table 1 are the values of the electromechanical coupling coefficient k_{t} at temperatures of 25 ℃, 30 ℃, 35 ℃, 40 ℃, 45 ℃, 50 ℃, and 55 ℃. Figure 3 shows the results fitted with the following equation:

$$k_{\text{t}} = 0.51864 + 0.182 \times 10^{-2}T - 3.11429 \times 10^{-5}T^2, \tag{40}$$

where T is the temperature in Celsius. Figure 3 shows the absolute values (less than 0.002) of the residuals with respect to polynomial fitting at the different temperatures. The different behaviours of k_{t} and k_{33} varying with temperature are due to different vibration frequencies, which result in different mechanical boundary conditions. The k_{t} vibrator belongs to the mechanical clamping boundary condition (high frequency),[14] whereas the k_{33} vibrator belongs to the mechanical free condition (low frequency).

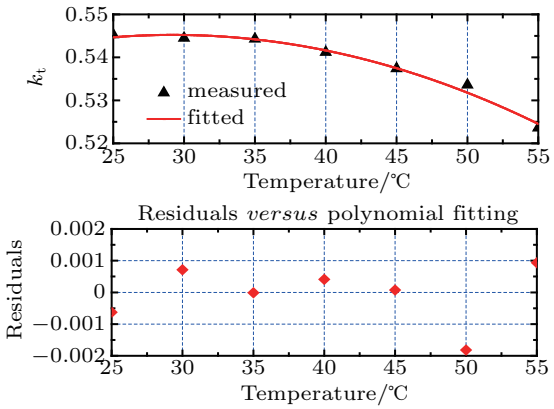


Fig. 3. Electromechanical coupling coefficient k_{t} at different temperatures.

Figures 4(a) and 4(b) show the relationship between resonant frequency constants and configuration ratio for the rectangular vibrator at temperatures of 25 ℃ and 55 ℃, respectively.

For a given configuration ratio G, f_1H and f_2H represent the two types of resonant frequency constants for the two-dimensional coupled vibration. For the rectangular piezoelectric vibrator, the point $\frac{1}{2}(G^{f_HH=f_LH} + G^{f_hH=f_lH})$ is defined as the 'mode dividing point'; when $M_1 = 1$, $G^{f_HH=f_LH} =$

$G^{f_hH=f_lH}$. By comparing Figs. 4(a) and 4(b), we find that the mode dividing point moves toward the lower configuration ratio G with temperature increasing as shown in Table 2. The coupling constant Γ_1 is approximately 0.85 in a temperature range of 25 ℃–55 ℃. From Table 2, we find that the applicability index (M_1) values are close to 1, indicating the applicability of the coupling theory for the rectangular piezoelectric single-crystal vibrator studied in this work.[8,9]

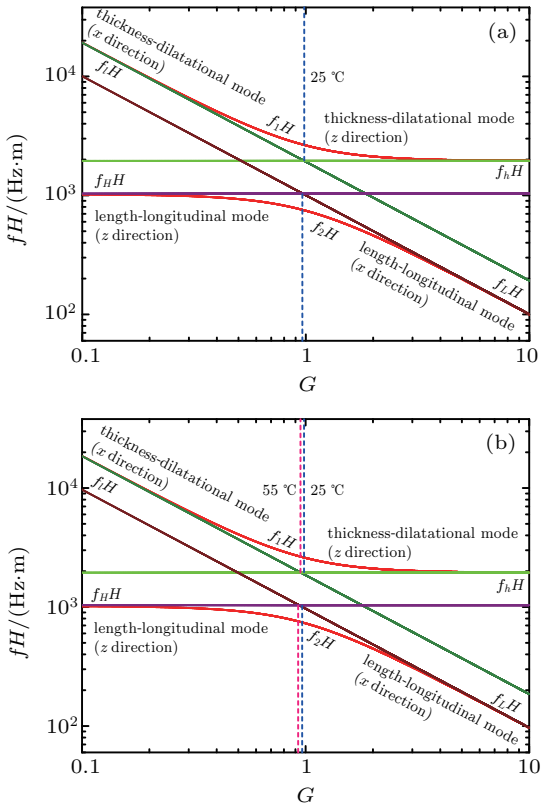


Fig. 4. Plot of resonant frequency constant *versus* configuration ratio for the rectangular piezoelectric vibrator at temperatures of (a) 25 ℃ and (b) 55 ℃, with straight lines indicating limiting frequency constants.

Figures 5(a) and 5(b) show the relationships between the resonant frequency constants and the configuration ratio for the cylindrical resonator at temperatures of 25 ℃ and 55 ℃, respectively. For the cylindrical piezoelectric vibrator, the point $\frac{1}{2}(G^{f_tH=f_rH}+G^{f_TH=f_RH})$ is the 'mode dividing point'; when $M_2=1$, $G^{f_tH=f_rH}=G^{f_TH=f_RH}$. By comparing Figs. 5(a) and 5(b), we find that the mode dividing point moves toward the greater configuration ratio G with temperature increasing as shown in Table 2. At 25 ℃, $G\approx 1.381$ and $k^{\mathrm{eff}}=0.7511$; at 40 ℃, $G\approx 1.399$ and $k^{\mathrm{eff}}=0.7509$; at 55 ℃, $G\approx 1.428$ and $k^{\mathrm{eff}}=0.7452$. The electromechanical coupling coefficient k^{eff} at the mode dividing point exhibits a decreasing trend with temperature increasing. The configuration ratio G for the rectangular bar and the cylindrical resonator are defined as $G=L/H$ and $G=H/R$, respectively; however, the poling direction for each of the two cases is along the height H as shown in Fig. 1. The coupling constant Γ_2 is approximately 0.89 in the temperature range of 25 ℃–55 ℃. From Table 2, we find that the applicability index M_2 is approximately 1.010. Therefore, like the scenario in the case of the rectangular bar, the coupling theory can also be applied to the cylindrical resonator.

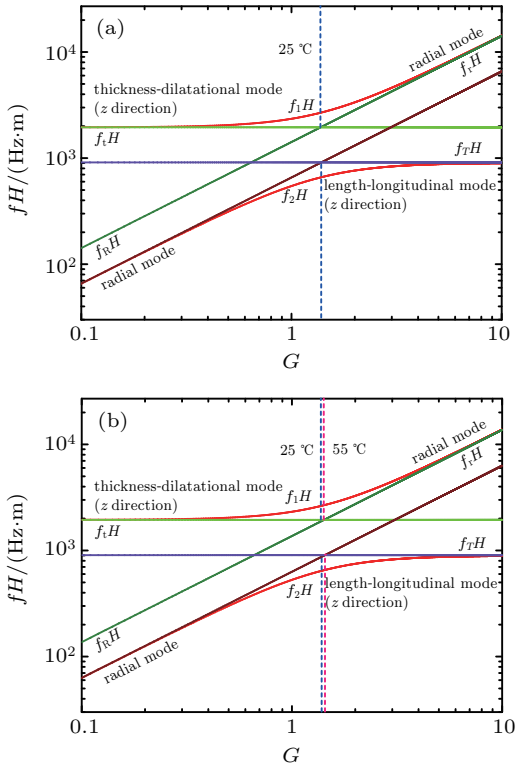


Fig. 5. Plots of resonant frequency constant against configuration ratio for cylindrical resonator at temperatures of (a) 25 ℃ and (b) 55 ℃, with straight lines indicating limiting frequency constants.

For both types of piezoelectric vibrators, the frequency constant f_1H is greater than f_2H as shown in Figs. 4 and 5, and hence, when $G\to 0$ or $G\to\infty$, f_1H approaches to the two limiting resonant frequency constants of the lower dimension, and f_2H approaches to the constants of the higher dimension. In other words, for the rectangular bar, when $G\to 0$, then $f_1H\to f_lH$ and $f_2H\to f_HH$, and when $G\to\infty$, then $f_1H\to f_hH$ and $f_2H\to f_LH$; for the cylindrical resonator, when $G\to 0$, then $f_1H\to f_tH$ and $f_2H\to f_RH$, and when $G\to\infty$, then $f_1H\to f_rH$ and $f_2H\to f_TH$. There is a very strong coupling between the resonant frequency along the poling direction (z direction) and that in the direction perpendicular to the poling direction (x or radial direction) when the configuration ratio G is close to the 'mode dividing point'. From Table 2, we find that the coupling constant Γ_2 of the cylindrical resonator is slightly greater than Γ_1 of the rectangular bar at a given temperature. The coupling constant Γ is not obviously dependent on temperature. This is because in Eqs. (6), (28), and (35), the elastic constants c_{11}^{E}, c_{12}^{E}, c_{13}^{E}, and c_{33}^{E} obtained from Ref. [4] vary with temperature. The elastic constants c_{11}^{E}, c_{12}^{E}, and c_{13}^{E} decrease with temperature increasing, whereas c_{33}^{E} is largely invariant in the temperature range of 25 ℃–55 ℃. Compared with that of the rectangular piezoelectric vibrator, the applicability index M_2 of the cylindrical vibrator is close

to 1 in the temperature range of 25 ℃–55 ℃ as shown in Table 2. Thus, in the application of the coupling theory, the internal consistency for the cylindrical resonator is slightly better than that for the rectangular bar. The applicability index M_2 of the cylindrical resonator is closer to 1 than the applicability index M_1 of rectangular bar, which results in the absolute value of ± 0.003, lower than that of the rectangular bar (± 0.004) as shown in Table 2.

Table 2. Values of coupling constant Γ, mode dividing point, and applicability index M at different temperatures.

Temperature/℃	Rectangular bar			Cylindrical resonator		
	Γ_1	Mode dividing point ($G = L/H$)	M_1	Γ_2	Mode dividing point ($G = H/R$)	M_2
25	0.8522	0.9756 ± 0.004	1.0165	0.8862	1.3805 ± 0.003	1.0078
30	0.8532	0.9714 ± 0.004	1.0180	0.8873	1.3852 ± 0.003	1.0083
35	0.8539	0.9673 ± 0.004	1.0172	0.8879	1.3914 ± 0.003	1.0074
40	0.8536	0.9626 ± 0.004	1.0184	0.8880	1.3989 ± 0.003	1.0081
45	0.8533	0.9567 ± 0.004	1.0184	0.8879	1.4073 ± 0.003	1.0076
50	0.8534	0.9520 ± 0.004	1.0191	0.8880	1.4144 ± 0.003	1.0079
55	0.8524	0.9435 ± 0.004	1.0198	0.8876	1.4279 ± 0.003	1.0085

4. Conclusions

In this work, we discuss the influence of temperature on 2D mode coupling effect and electromechanical coupling coefficient of cylindrical $[001]_c$-poled Mn-doped 0.24PIN–0.46PMN–0.30PT piezoelectric single-crystal vibrator with an arbitrary configuration ratio. For the cylindrical resonator, the effective electromechanical coupling coefficient k^{eff} at the mode dividing point exhibits a decreasing trend with temperature increasing. The electromechanical coupling coefficient k_t decreases with temperature increasing, whereas the electromechanical coupling coefficient k_{33} is largely invariant in a temperature range of 25 ℃–55 ℃. With temperature increasing, the shift in the mode dividing point increases the scale of the poling direction. For a given vibrator, the temperature has little effect on coupling constant Γ in the range of 25 ℃–55 ℃. However, the geometry of the piezoelectric vibrator affects the coupling constant. For a given temperature, the coupling constant Γ of the cylindrical resonator is slightly greater than that of the rectangular bar. In a temperature range from 25 ℃ to 55 ℃, the applicability index values of the two piezoelectric vibrators are both close to 1, indicating that the coupling theory can be applied to piezoelectric vibrators made of late-model piezoelectric single crystals, considering temperature fluctuations.

References

[1] Zhang S, Luo J, Hackenberger W, Sherlock N P, Jr R J and Shrout T R 2009 *J. Appl. Phys.* **105** 104506
[2] Qiao L, Li Q, Qiu C, Liu Y, Liu J, Xu Z and Li F 2019 *IEEE Trans. Ultrason. Ferroelectr. Freq. Control* **66** 1786
[3] Yan T L, Chen B, Liu G, Niu R P, Shang J, Gao S, Xue W H, Jin J, Yang J R and Li R W 2017 *Chin. Phys. B* **26** 067702
[4] Tang L, Tian H, Zhang Y and Cao W 2016 *Appl. Phys. Lett.* **108** 082901
[5] Wu J, Gao X, Chen J, Wang C, Zhang S and Dong S 2018 *Acta Phys. Sin.* **67** 207701 (in Chinese)
[6] You J, Guan C and Zhou H 2017 *Chin. Phys. B* **26** 054215
[7] Wang W, Or S W and Luo H 2017 *Crystals* **7** 101
[8] Onoe M and Tiersten H F 1963 *IEEE Trans. Ultrason. Eng.* **10** 32
[9] Ikeda T 1990 *Fundamentals of Piezoelectricity* (Oxford: Oxford University Press) pp. 116–118
[10] Lamberti N and Pappalardo M 1995 *IEEE Trans. Ultrason. Ferroelectr. Freq. Control* **42** 243
[11] Kim M, Kim J and Cao W 2006 *J. Appl. Phys.* **99** 074102
[12] Kim M, Kim J and Cao W 2005 *Appl. Phys. Lett.* **87** 132901
[13] Huang N, Zhang R and Cao W 2007 *Appl. Phys. Lett.* **91** 122903
[14] Chen C W, Xiang Y, Tang L G, Cui L, Lin B Q, Du W D and Cao W W 2019 *Chin. Phys. B* **28** 127702